This article has been accepted for publication in a future issue of this journal, but has not been fully edited. Content may change prior to final publication. Citation information: DOI 10.1109/TMECH.2019.2917448, IEEE/ASME Transactions on Mechatronics

Control Synthesis and ISS Stability Analysis of Dual-User Haptic Training System Based on S-Shaped Function

Mohammad Motaharifar, *Student Member, IEEE,* Hamid D. Taghirad, *Senior Member, IEEE,* Keyvan Hashtrudi-Zaad, *Senior Member, IEEE,* and Seyed Farzad Mohammadi

***Abstract*—The controller design and stability analysis of dual user training haptic system is studied. Most of the previously proposed control methodologies for this system have not simultaneously considered special requirements of surgery training and stability analysis of the nonlinear closed loop system which is the objective of this paper. In the proposed training approach, the trainee is allowed to freely experience the task and be corrected as needed, while the trainer maintains the task dominance. A special S-shaped function is suggested to generate the corrective force according to the magnitude of motion error between the trainer and the trainee. The closed loop stability of the system is analyzed considering the nonlinearity of the system components using the Input-to-State Stability (ISS) approach. Simulation and experimental results show the effectiveness of the proposed approach.**

***Index Terms*—Haptics, Surgery Training, Dual-User, S-Shaped Function, Input-to-State Stability Analysis.**

I. Introduction

OVER the past few decades, surgical instrumentation, techniques and types have progressed by leaps and bounds [1], [2]. As an example, surgical robots such as da Vinci, provide higher level of maneuverability and accuracy for performing minimally invasive surgery (MIS) [3]. However, surgical training, which follows more traditional manual methods, lags this process and faces challenges such as unanticipated mistakes made by the trainee which may lead to undesirable complications for the patients [4].

Haptic technology has been harnessed for the design of robotic-based medical simulators for training MIS [5], dental procedures [6], and sonography [7]. Recently, dual-user haptic systems consisting of two haptic interfaces, one for the trainer and one for the trainee, has emerged as a viable surgical training apparatus [8]. In these systems, the trainer and the trainee collaboratively perform surgical tasks through their haptic interfaces or consoles.

This work was supported in part by the National Institute for Medical Research Development under Grant NO. 942314

Mohammad Motaharifar and Hamid D. Taghirad are with the Advanced Robotics and Automated Systems (ARAS), Industrial Control Center of Excellence, Faculty of Electrical Engineering, K. N. Toosi University of Technology, Tehran 1969764499, Iran (e-mail: motaharifar@email.kntu.ac.ir, taghirad@kntu.ac.ir).

Keyvan Hashtrudi-Zaad is with the Department of Electrical and Computer Engineering, Queen's University, Kingston, ON K7L 3N6, Canada (e-mail: khz@queensu.ca)

Seyed Farzad Mohammadi is with the Translational Ophthalmology Research Center, Farabi Eye Hospital, Tehran University of Medical Sciences, Tehran, 1336616351, Iran. (e-mail: sfmohammadi@tums.ac.ir)

The paramount importance for the design of controllers for such systems are user-task interaction stability under various operational conditions, and satisfactory surgical task performance. To this effect, several control architectures have been proposed for dual-user haptic systems. A number of these controllers have been designed for generic human haptic guidance applications [9], while others focus on the surgical or training nature of the collaboration [10]–[12]. Nudehi introduced *dominance factor* which determines the dominance of each user over the task [10]. The choice of the control architecture has been researched actively within the past few years. Khademian et al. proposed multilateral shared control architecture with dominance factor that provides kinesthetic feedback from the environment [11]. In [12], a similar architecture have been utilized to develop impedance control for a multi-master cooperative haptic system.

Although the above methodologies entertain key novel concepts in shared control for dual-user haptic systems, by and large they face a number of shortcomings that need to be addressed: (i) In several control architectures, a guidance force linearly related to the position error between the trainer and the trainee is exerted to the trainee's hand [10]–[12]. As a result, the guidance force is applied to the trainee's hands for any small position error without considering a safe region within which the trainee is allowed to move her/his hand freely for increased independence. In those approaches the total force felt by the trainee is a combination of the guidance force and the environmental forces. This constitutes an important drawback of those control architectures as the trainee cannot distinguish between the environmental forces and guidance forces; (ii) Other control architectures have been proposed to mitigate the above problems, for example by allowing the trainee's hand to move freely inside a spherical free region centered at the trainer's position at any time [13]. However, the stability of these systems is not systematically analyzed by considering nonlinearity of the system dynamics and the switching nature of the control architecture; (iii) The situation where a large position error occurs between the trainer and the trainee have seldom been considered in a systematic manner. An important fact is that, large position error may compromise the stability in real experiments due to actuator saturation. Time Domain Passivity Approach (TDPA) has been utilized for guaranteed coupled stability for dual-user systems [14] and multi-master/multi-slave systems [15]. While the focus of these works are on dealing with time-delays, they have

This article has been accepted for publication in a future issue of this journal, but has not been fully edited. Content may change prior to final publication. Citation information: DOI 10.1109/TMECH.2019.2917448, IEEE/ASME Transactions on Mechatronics

not explicitly considered the special requirements of training systems such as safe region and large position error.

The major contribution of this work is developing a control structure that is customized for surgery training applications and addresses the above shortcomings. Our training approach is based on allowing the trainee to freely experience the task and be corrected as needed, while the trainer maintains the task dominance. To this purpose, the controller implements three modes of operation, namely *trusting mode*, *guidance mode*, and *large error mode*. These modes are seamlessly implemented through an S-shaped function that converts the position error between the trainer and the trainee to the trainee's corrective force. The stability of the closed-loop system is analyzed using Input-to-State (ISS) stability analysis method that takes into account the dynamic nonlinearities in the haptic consoles and the proposed controller.

The rest of this paper is organized as follows. The dual user haptic system and its control objectives are described in Section II. The dynamics of the system is explained in Section III. The proposed control structure is detailed in Section IV. Section V investigates the stability analysis of the closed loop system. Simulation and experimental results are presented in Section VI, and the concluding remarks are stated in Section VII.

II. The Proposed Haptic System

Figure 1 illustrates our proposed dual-user haptic system for surgery training. The system is composed of three main components: the trainer haptic console #1, the trainee haptic console #2, and the virtual environment. The trainer and the trainee are interfaced with their respective consoles to perform the surgical operation. The surgery is directly performed on the virtual environment by the trainer and the trainee learns the skills through the haptic feedback received from the trainer and the environment. In other words, this structure is based on allowing the trainee to experience the sense of surgical operation and receive the haptic guidance from the trainer while the task dominance is maintained by the trainer. While there are collaborative control architectures for trajectory training with position coupling in shared virtual environment [11], the proposed system is more suitable for the most primary level of training in which the trainee does not have sufficient experience to perform the operation. Therefore, the operation is performed by the trainer, and the forces of the virtual environment depend on the trainer's interaction with the environment. Here, both the trainer and the trainee receive the environment force through their haptic consoles. The commands exerted by the trainer are implemented on the console #2 according to an S-shape nonlinear function which will be introduced later.

The main application of the proposed haptic system is intraocular eye surgery with limited workspace such as Cataract and vitrectomy. Note that, the required precision for those surgical operations is about hundred micron which is achievable for the surgeons after several years of continuous practice. As mentioned earlier, the objective is to use this training philosophy for the initial stages of training in order to accelerate

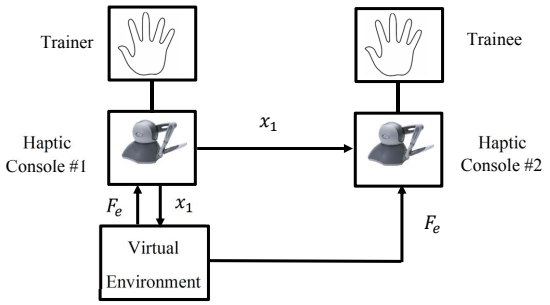

Fig. 1: The haptic system for surgery training.

the pace and the efficiency of training. It should be noted that the above training philosophy can also be extended to remote training with physical phantoms, cadavers and patients where the environment forces are felt by the trainer and the measured forces are applied to the trainee through the haptic console #2.

The control structure is designed to guarantee coupled stability and provide pose correction for the trainee as necessary. The motions of the trainer, the expert surgeon, are trusted and do not need to be corrected. As a result, only a stabilizing controller is required for the haptic console #1. On the other hand, the movements of the trainee are not always trusted and corrective guidance from the trainer is sometimes necessary. The controller for console #2 is designed to implement the following modes of operation:

- *Trusting mode:* In this mode, the trainee's movements are trusted, and as such no intervention is required from the trainer. This is a situation where the motion error between the trainee and the trainer is less than a predefined value. The most important feature of trusting mode is that the trainee is able to freely move within a safe region without any interference from the trainer. In this mode the role of the haptic system is to recreate the sense of touch for the trainee. The size of the safe region is determined by the safety margin of the surgical procedure.
- *Guidance mode:* In this mode, the motion error between the trainer and the trainee exceeds the predefined safety threshold. As a result, the trainee needs haptic guidance from the trainer to perform the tasks. The nature of the corrective force is to guide the trainee to loosely follow the trainer's trajectory (in guidance mode) and to provide an opportunity to the trainee to increasingly perform independently as the trainee acquires the necessary skills.
- *Large error mode:* This mode happens if the motion error between the trainee and the trainer becomes too large, which may lead to considerable amount of control signal and damage to the actuators. In order to make sure that the proposed structure does not demand too much from the actuators, the actuator saturation should be considered in the control architecture.

In this paper, an S-shaped function is proposed to realize the above operating modes. The control structure will be introduced and analyzed in the Section IV.

This article has been accepted for publication in a future issue of this journal, but has not been fully edited. Content may change prior to final publication. Citation information: DOI 10.1109/TMECH.2019.2917448, IEEE/ASME Transactions on Mechatronics

III. System Dynamics

Consider n-Dof manipulators with non-redundant kinematics and $n \leq 6$ for the consoles 1 and 2 represented by the following dynamic equation [16]

$$M_i(q_i)\ddot{q}_i + C_i(q_i, \dot{q}_i)\dot{q}_i + G_i(q_i) = u_i + J_i^T(q_i)f_{hi} \quad (1)$$

where $q_i \in \mathbb{R}^{n\times 1}$ are position vectors in joint space, $M_i(q_i) \in \mathbb{R}^{n\times n}$ are the inertia matrices, $C_i(\dot{q}_i, q_i) \in \mathbb{R}^{n\times n}$ are the centrifugal and Coriolis matrices, $G_i(q_i) \in \mathbb{R}^{n\times 1}$ are the gravity vectors, $u_i \in \mathbb{R}^{n\times 1}$ are the control torque vectors, $J_i(q_i) \in \mathbb{R}^{n\times n}$ are the Jacobian matrices and $f_{hi} \in \mathbb{R}^{n\times 1}$ are the vector of forces exerted by human operators for $i = 1, 2$ where the subscript i denotes the haptic console #1 for $i = 1$ and haptic console #2 for $i = 2$.

The dynamic equation (1) benefits from the following properties that will be used for stability analysis [16]:

Property 1. The inertia matrix $M_i(q_i)$ is a symmetric positive definite matrix.

Property 2. The matrix $\dot{M}_i(q_i) - 2C_i(q_i, \dot{q}_i)$ is skew symmetric, i.e. $v^T\big(\dot{M}_i(q_i) - 2C_i(q_i, \dot{q}_i)\big)v = 0 \forall v \in \mathbb{R}^n$, provided that $C(q_i, \dot{q}_i)$ is in Christoffel form. Otherwise, it is valid only for $v = \dot{q}_i$.

We assume the position of the end effectors of the haptic consoles $x_i =\in \mathbb{R}^{n\times 1}$ are available through the forward kinematics relation [16]

$$x_i = k_i(q_i) \quad (2)$$

where $k_i(.)$ is a nonlinear function expressing the relationship between joint space and task space generalized position. Besides, the Jacobian matrix $J_i(q_i) \in \mathbb{R}^{n\times n}$ determines the relationship between the task space velocity $\dot{x}_i \in \mathbb{R}^{n\times 1}$ and the joint space velocity $\dot{q}_i$ according to

$$\dot{x}_i = J_i(q_i)\dot{q}_i. \quad (3)$$

Differentiating (3) with respect to time yields the task space acceleration, $\ddot{x}_i \in \mathbb{R}^{n\times 1}$, in terms of joint positions and velocities as

$$\ddot{x}_i = J_i(q_i)\ddot{q}_i + \dot{J}_i(q_i)\dot{q}_i. \quad (4)$$

Furthermore, the following assumptions are made throughout the paper concerning the forces applied by the environment and the operators' hands.

Assumption 1. The environment is assumed to be a passive system, that is,

$$\int_0^t \dot{x}_1 f_e d\tau \geq 0 \quad \forall t \geq 0. \quad (5)$$

where $f_e = f_e(x_1, \dot{x}_1)$ denotes the environment force, which is presumed to satisfy Lipschitz continuity condition for both its variables [17].

Assumption 2. The operators' hand dynamics are modeled by the following linear time-invariant mass-damper-spring systems [9], [18]

$$f_{hi} = f_{hi}^* - M_{hi}\ddot{x}_i - B_{hi}\dot{x}_i - K_{hi}x_i \quad (6)$$

where f_{hi}^* is the exogenous force generated by the operator #i and M_{hi}, B_{hi}, and K_{hi} are constant, symmetric, and positive definite matrices corresponding to mass, damping, and stiffness of the operator #i, respectively.

IV. The Proposed Control Architecture

As already explained, the haptic console #1 is controlled by the trainer, while the haptic console #2 is held by the trainee. The trainer does not need any position feedback from the trainee. As a result, the following conventional "PD+gravity compensation" algorithm in task space combined with the force reflection term is utilized for the haptic console #1:

$$u_1 = G_1(q_1) + J_1^T(q_1)f_e - J_1^T(q_1)(K_{P1}x_1 + K_{D1}\dot{x}_1) \quad (7)$$

where $K_{P1} \in \mathbb{R}^{n\times n}$ and $K_{D1} \in \mathbb{R}^{n\times n}$ are symmetric and positive definite matrices. The matrices K_{P1} and K_{D1} are local stiffness and damping gains. While local damping improves stability, local stiffness causes a centering force to be applied to the haptic console #1. As will be shown in proposition 1, the exitance of the positive-definite K_{P1} is essential to guarantee the positive definiteness of the Lyapunov function V_1 for the haptic console #1. Having said that high stiffness gain of the local control parameter increases the centering force to the trainer's hands and can impose adverse effect on the performance of the haptic system.Therefore, this gain is selected small to limit the centering force applied to the trainer's hand. Also note that, the proposed architecture only requires the gravity information from the system dynamics, the parameters of which can be estimated using simple off-line methods. On the other hand, the following control law which is a combination of gravity compensation, force reflection, and a novel guidance term is considered for the haptic console #2:

$$\begin{aligned} u_2 =& G_2(q_2) + J_2^T(q_2)f_e \\ & - J_2^T(q_2)(K_{P2}\phi(x_2 - x_1) + K_{D2}\dot{x}_2) \end{aligned} \quad (8)$$

where $K_{P2} \in \mathbb{R}^n$ and $K_{D2} \in \mathbb{R}^n$ are symmetric and positive definite matrices, and $\phi(\theta)$ is a special function depicted in Fig. 2. Having the shape of an S letter in each half of the Cartesian plane, $\phi(\theta)$ is referred to as the S-shaped function.

The S-shaped function is the proposed solution for realizing the three aforementioned operating modes. This function generates the corrective force according to the magnitude of the trainee's motion error. As shown in Fig. 2, the S-shaped function is characterized by the three dead-zone, knee, and saturation regions. The dead-zone region realizes the trusting mode by outputting negligible corrective forces when the motion error of the trainee is smaller than the safe threshold of the surgery. The knee region implements the guidance mode by producing non-zero corrective forces when the trainee's error goes beyond the safe threshold. When the error goes beyond the maximum threshold, the corrective force is saturated to a fixed value to ensure stability, realizing the large error mode.

In addition to realizing the three mentioned operating regions, the following assumption set on the S-shaped function $\phi(\theta)$ are considered for stability analysis [19].

This article has been accepted for publication in a future issue of this journal, but has not been fully edited. Content may change prior to final publication. Citation information: DOI 10.1109/TMECH.2019.2917448, IEEE/ASME Transactions on Mechatronics

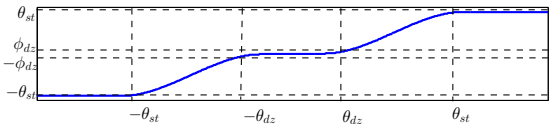

Fig. 2: The S-shaped function, $\phi(\theta)$.

Assumption 3. The S-shaped function, $\phi(\theta)$ is presumed to satisfy the following properties:

1) $\phi(\theta)$ is continuously differentiable.
2) $\phi(\theta)$ is the derivative of a positive function $\Phi(\theta)$, i.e., $\phi(\theta) = \frac{d\Phi(\theta)}{\theta}$ where $\Phi(\theta) > 0 \quad \forall \theta \neq 0$ and $\phi(0) = 0$.
3) A positive constant exists c such that $c\phi^2(\theta) \leq \Phi(\theta)$.

An example of such a function can be given in the following form

$$\phi(\theta) = \begin{cases} -\theta_{st}, & \theta \leq -\theta_{st} \\ F_N(\theta), & -\theta_{st} \leq \theta \leq -\theta_{dz} \\ \frac{\phi_{dz}}{\theta_{dz}^2}\theta|\theta|, & -\theta_{dz} \leq \theta \leq \theta_{dz} \\ F_P(\theta), & \theta_{dz} \leq \theta \leq \theta_{st} \\ \theta_{st}, & \theta \geq \theta_{st} \end{cases}$$

where θ_{dz} and θ_{st} are the dead-zone and saturation parameters, which are also illustrated in Figure 2. The parameter θ_{dz} represents the width of the dead-zone region and is determined by the safety threshold of the surgery, whereas the parameter θ_{st} is determined by the maximum control effort of the robots. The parameter ϕ_{dz} is the maximum value of the output in the dead-zone region, which should be chosen a small number in order that the output of the dead-zone region becomes negligible. The smooth functions $F_i, i = \{N, P\}$ may be set as cubic polynomials such as $F_i = f_{i0} + f_{i1}\theta + f_{i2}\theta^2 + f_{i3}\theta^3$ where subscripts N and P represent the polynomials for the negative and positive parts of the plane. Substituting for the value of the output and its derivative at θ_{dz} and θ_{st}, the following matrix equation is obtained to compute the polynomial parameters:

$$\begin{bmatrix} f_{i0} \\ f_{i1} \\ f_{i2} \\ f_{i3} \end{bmatrix} = \begin{bmatrix} \kappa & \theta_{dz} & \kappa\theta_{dz}^2 & \theta_{dz}^3 \\ \kappa & \theta_{st} & \kappa\theta_{st} & \theta_{st} \\ 0 & \kappa & 2\theta_{dz} & 3\kappa\theta_{dz}^2 \\ 0 & \kappa & 2\theta_{st} & 3\kappa\theta_{st}^2 \end{bmatrix}^{-1} \begin{bmatrix} \phi_{dz} \\ \phi_{st} \\ \frac{2\kappa\phi_{dz}}{\theta_{dz}} \\ 0 \end{bmatrix}$$

where $\kappa = 1$ for $i = P$ and $\kappa = -1$ for $i = N$. The determinant of the above 4×4 matrix is $(\theta_{st} - \theta_{dz})^4$ meaning that this matrix is invertible if $\theta_{st} \neq \theta_{dz}$.

V. Stability Analysis

Our approach for stability analysis is to first prove the stability of each subsystem, and then analyze the stability of the entire system. To find suitable Lyapunov function candidates for each subsystem, the inner product approach, which has been widely used in robotics, is utilized [19]. The Input-to-State (ISS) stability analysis methodology is then employed to study the stability of the closed-loop system. Next, we will introduce the concept of ISS.

Definition 1: [20] Consider the system

$$\dot{x} = f(x, u) \tag{9}$$

where $f : D_x \times D_u \to \mathbb{R}^n$ is locally Lipschitz in x and u. The sets D_x and D_u are defined by $D_x = \{x \in \mathbb{R}^n : \|x\| < r_x\}$, $D_u = \{u \in \mathbb{R}^m : \|u\| < r_u\}$, in which r_x and r_u are the radii of D_x and D_u, respectively. The system (9) is ISS if there exists a class $\mathcal{KL}$ function β and a class $\mathcal{K}$ function γ such that for any initial state x_0 and any bounded input the following inequality is satisfied:

$$\|x(t)\| \leq \beta(\|x_0\|, t) + \gamma(\|u_T(t)\|_\infty), \qquad 0 \leq t \leq T.$$

Theorem 1 connects the concept of ISS presented in Definition 1 to the Lyapunov theory, and forms the analysis framework for this section.

Theorem 1 [20]: The system (9) is ISS in the sense of Definition 1, provided that there exists a continuously differentiable function $V : D \to \mathbb{R}$ such that

$$\alpha_1(\|x\|) \leq V(x) \leq \alpha_2(\|x\|)$$
$$\dot{V}(x) \leq -\alpha_3(\|x\|) + \sigma(\|u\|)$$

where $\dot{V}$ is the derivative of V along the trajectory solutions of the system (9) and α_1, α_2, α_3, and σ are class $\mathcal{K}$ functions.

Next, we will take a look at the the well-known Young's quadratic inequality.

Lemma 1 [21]: For any vector x and y, and $\epsilon > 0$, the following inequality is satisfied:

$$|x^T y| \leq (\frac{\epsilon}{2})\|x\|^2 + (\frac{1}{2\epsilon})\|y\|^2.$$

The ISS stability of the haptic console#1 is now analyzed.

Proposition 1: The closed-loop subsystem "haptic console #1 + environment" is ISS with state $[x_1^T, \dot{x}_1^T]^T$ and input f_{h1}^*.

Proof: By substituting the control law (7) into the dynamic equation (1) and using (3), (4) and(6), the following closed-loop system is obtained

$$\begin{aligned} &(M_{x1}(q_1) + M_{h1})\ddot{x}_1 + (C_{x1}(q_1, \dot{q}_1) + B_{h1} + K_{D1})\dot{x}_1 \\ &(K_{h1} + K_{P1})x_1 = f_{h1}^* - f_{e1} \end{aligned} \tag{10}$$

where

$$\begin{aligned} M_{x1}(q_1) &= J_1^{-T}(q_1)M_1(q_1)J_1^{-1}(q_1) \\ C_{x1}(q_1, \dot{q}_1) &= J_1^{-T}(q_1)C_1(q_1, \dot{q}_1)J_1^{-1}(q_1) \\ &\quad - M_{x1}(q_1)\dot{J}_1(q_1)J_i^{-1}(q_1). \end{aligned}$$

It is easy to conclude that Property 1 and Property 2 hold for $M_{x1}(q_1)$ and $C_{x1}(q_1, \dot{q}_1)$ [16]. Taking an inner product between $\dot{x}_1$ and (10) and using the skew symmetry property of the matrix $\dot{M}_{x1}(q_1) - 2C_{x1}(q_1, \dot{q}_1)$ results in

$$\frac{d}{dt}V_1(x_1, \dot{x}_1) = -\dot{x}_1^T(B_{h1} + K_{D1})\dot{x}_1 + \dot{x}_1^T f_{h1}^* \tag{11}$$

in which,

$$\begin{aligned} V_1(x_1, \dot{x}_1) =& \frac{1}{2}\dot{x}_1^T(M_{x1}(q_1) + M_{h1})(q_1)\dot{x}_1 \\ &+ \frac{1}{2}x_1^T(K_{h1} + K_{P1})x_1 + \int_0^t \dot{x}_1 f_e d\tau. \end{aligned} \tag{12}$$

The positive definiteness property of $V_1(x_1, \dot{x}_1)$ can be concluded from Property 1 and (5). Now, utilizing Lemma 1, it is

This article has been accepted for publication in a future issue of this journal, but has not been fully edited. Content may change prior to final publication. Citation information: DOI 10.1109/TMECH.2019.2917448, IEEE/ASME Transactions on Mechatronics

easy to show that the time derivative of $V_1(x_1, \dot{x}_1)$ is upper-bounded, that is

$$\begin{aligned}\frac{d}{dt}V(x_1,\dot{x}_1) \leq &-\frac{3}{4}\lambda_{\min}(B_{h1}+K_{D1})\|\dot{x}_1\|^2 \\ &+\frac{1}{\lambda_{\min}(B_{h1}+K_{D1})}\|f_{h1}^*\|^2.\end{aligned} \tag{13}$$

From (12) and (13), the haptic console #1 subsystem is ISS with respect to state $[x_1^T, \dot{x}_1^T]^T$ and the input F_{h1}^*. □

The next step is to investigate the ISS stability of the haptic console #2 as presented in Proposition 2.

Proposition 2: The closed-loop subsystem of the haptic console #2 is ISS with respect to the state $[x_2^T, \dot{x}_2^T]^T$ and the input $[x_1^T, \dot{x}_1^T, f_{h2}^{*T}]^T$.

Proof: If the control law (8) is included within the dynamic equation (1), the resulting closed-loop system is

$$\begin{aligned}&(M_{x2}(q_2)+M_{h2})\ddot{x}_2+(C_{x2}(q_2,\dot{q}_2)+B_{h2})\dot{x}_2 \\ &+K_{D2}\dot{x}_2+K_{h2}x_2+K_{P2}\phi(\tilde{x})=f_{h2}^*+f_e\end{aligned} \tag{14}$$

where $\tilde{x} = x_2 - x_1$. We define $r = \dot{x}_2 + \gamma\phi(\tilde{x})$ with a small and positive scalar γ, and take an inner product between r and (14) and use the skew symmetric property of the matrix $\dot{M}_{x2}(q_2) - 2C_{x2}(q_2, \dot{q}_2)$ to obtain

$$\begin{aligned}\frac{d}{dt}V_2(\tilde{x},\dot{x}_2) =& -\gamma\phi(\tilde{x})^T K_{P2}\phi(\tilde{x}) \\ &-\dot{x}_2^T(K_{D2}+B_{h2})\dot{x}_2 \\ &-\gamma\phi(\tilde{x})^T(-\dot{M}_{x2}(q_2)+C_{x2}(q_2,\dot{q}_2))\dot{x}_2 \\ &-\gamma\dot{\phi}(\tilde{x})^T(M_{x2}(q_2)+M_{h2})\dot{x}_2 \\ &-\dot{x}_1^T(K_{P2}+\gamma K_{D2}+\gamma B_{h2})\phi(\tilde{x}) \\ &-\gamma\phi(\tilde{x})^T K_{h2}(\tilde{x}+x_1) \\ &+\dot{x}_2^T(f_{h2}^*+f_e)+\gamma\phi(\tilde{x})^T(f_{h2}^*+f_e)\end{aligned} \tag{15}$$

where

$$\begin{aligned}V_2(\tilde{x},\dot{x}_2) =& \frac{1}{2}\dot{x}_2^T(M_{x2}(q_2)+M_{h2})\dot{x}_2 \\ &+\sum_{i=1}^{n}k_{p2i}\Phi_i(\tilde{x})+x_2^T K_{h2}x_2 \\ &+\gamma\phi(\tilde{x})^T(M_{x2}(q_2)+M_{h2})\dot{x}_2 \\ &+\sum_{i=1}^{n}\gamma(k_{d2i}+b_{h2i})\Phi_i(\tilde{x})\end{aligned} \tag{16}$$

and k_{p2i}, k_{d2i}, and b_{h2i} stand for the ith diagonal elements of K_{p2}, K_{d2}, and B_{h2}, respectively. It is easy to show that

$$\begin{aligned}&\frac{1}{8}\dot{x}_2^T(M_{x2}(q_2)+M_{h2})\dot{x}_2+\sum_{i=1}^{n}\gamma(k_{d2i}+b_{h2i})\Phi_i(\tilde{x}) \\ &+\gamma\phi(\tilde{x})^T(M_{x2}(q_2)+M_{h2})\dot{x}_2 \\ &\geq\sum_{i=1}^{n}\gamma\Big((k_{d2i}+b_{h2i})c-2\gamma\lambda_{\max}\big(M_{x2}(q_2)+M_{h2}\big)\Big)\phi_i^2(\tilde{x})\end{aligned} \tag{17}$$

where $\lambda_{\max}\big(M_{x2}(q_2)+M_{h2}\big)$ is the maximum eigenvalue of $M_{x2}(q_2)+M_{h2}$ for all q_2. Then, substituting (17) into (16) leads to

$$\begin{aligned}V_2(\tilde{x},\dot{x}_2) \geq &\frac{3}{8}\dot{x}_2^T M_{x2}(q_2)\dot{x}_2+\sum_{i=1}^{n}\Big(k_{p2i}\Phi_i(\tilde{x}) \\ &+\gamma\big((k_{d2i}+b_{h2i})c-2\gamma\lambda_{\max}(M_{x2}(q_2))\big)\phi_i^2(\tilde{x})\Big)\end{aligned} \tag{18}$$

which shows the positive definiteness of the Lyapunov candidate function $V_2(\tilde{x}, \dot{x}_2)$ for sufficiently small γ.

Next, the negative definiteness of the derivative of the Lyapunov candidate function (15) is analyzed. First, we take a look at the following term:

$$\begin{aligned}\Xi =& -\gamma\phi(\tilde{x})^T(-\dot{M}_{x2}(q_2)+C_{x2}(q_2,\dot{q}_2))\dot{x}_2 \\ &-\gamma\dot{\phi}(\tilde{x})^T(M_{x2}(q_2)+M_{h2})\dot{x}_2.\end{aligned} \tag{19}$$

Since $\dot{M}_{x2}(q_2)$, $C_{x2}(q_2, \dot{q}_2))$, and $\dot{\phi}(\tilde{x})$ are all linear functions of $\dot{x}_2$, it can be shown that Ξ is quadratic in $\dot{x}_2$ and bounded in the other variables [19]. As a result, there exists a positive real value ρ such that $\Xi \leq \rho\|\dot{x}_2\|^2$. Now, by using Lemma 1 is used for the cross terms and the resulted inequalities are combined with (15) and (19)to derive the following inequality:

$$\begin{aligned}\frac{d}{dt}V_2(\tilde{x},\dot{x}_2) \leq &-\beta_1(\|\tilde{x}\|)-\beta_2\|\dot{x}_2\|^2 \\ &+\beta_3\|x_1\|^2+\beta_4\|\dot{x}_1\|^2+\beta_5\|(f_{h2}^*+f_e)\|^2\end{aligned} \tag{20}$$

where $\beta_1(s)$ is a class $\mathcal{K}$ function and β_2, β_3, β_4, and β_5, are scalars expressed as

$$\begin{aligned}\beta_1(s) &= \frac{5}{8}\gamma\lambda_{\min}(K_{P2})\phi(s)^2+\gamma\lambda_{\min}(K_{h2})s\phi(s) \\ \beta_2 &= \frac{7}{8}\lambda_{\min}(K_{D2}+B_{h2})-\rho \\ \beta_3 &= \frac{4\lambda_{\max}^2(K_{h2})}{\lambda_{\min}(K_{p2})} \\ \beta_4 &= \frac{4\lambda_{\max}^2(K_{P2}+\gamma K_{D2})}{\gamma\lambda_{\min}(K_{P2})} \\ \beta_5 &= \frac{4}{\lambda_{\min}(K_{D2}+B_{h2})}+\frac{4\gamma}{\lambda_{\min}(K_{D2})}\end{aligned} \tag{21}$$

From (16) and (20) the closed-loop subsystem of the haptic console #2 is ISS with respect to state $[\tilde{x}^T, \dot{x}_2^T]^T$ and input $[\dot{x}_1^T, (f_{h2}^* - f_e)^T]^T$, for sufficiently small γ and sufficiently large K_{D2}. Using Assumption 1, it is possible to conclude that the haptic console #2 is also ISS with respect to state $[\tilde{x}^T, \dot{x}_2^T]^T$ and input $[x_1^T, \dot{x}_1^T, f_{h2}^*]^T$. □

The stability of cascade system as a tool for our final stability analysis is expressed in Lemma 2.

Lemma 2: [20] Consider the cascade system given by

$$\begin{aligned}\Sigma_1: &\quad \dot{\chi}_1 = f_1(\chi_1,\mu_1) \\ \Sigma_2: &\quad \dot{\chi}_2 = f_2(\chi_2,\chi_1,\mu_2)\end{aligned} \tag{22}$$

where Σ_1 is ISS with state χ_1 and input μ_1, and Σ_2 is ISS with state χ_2 and input $[\chi_1^T, \mu_2^T]^T$. Therefore, the cascade connection of the subsystems is ISS with state $[\chi_1^T, \chi_2^T]^T$ and input $[\mu_1^T, \mu_2^T]^T$.

Finally, the stability analysis of the entire haptic system as our main conclusion is investigated in Theorem 2. To this end,

This article has been accepted for publication in a future issue of this journal, but has not been fully edited. Content may change prior to final publication. Citation information: DOI 10.1109/TMECH.2019.2917448, IEEE/ASME Transactions on Mechatronics

Lemma 2 is applied to the system considering $\chi_1 = [x_1^T, \dot{x}_1^T]^T$, $\chi_2 = [\tilde{x}^T, \dot{x}_2^T]^T$, $\mu_1 = f_{h1}^*$, and $\mu_2 = f_{h2}^*$.

Theorem 2: The dual-user haptic training system (1), (7), and (8) is ISS with respect to the input $[f_{h1}^T, f_{h2}^T]^T$.

Proof: From Proposition 1, the subsystem of the haptic console #1 is ISS with state $[x_1^T, \dot{x}_1^T]^T$ and input f_{h1}^*. From Proposition 2 the subsystem of the haptic console #2 is ISS with respect to state $[x_2^T, \dot{x}_2^T]^T$ and input $[x_1^T, \dot{x}_1^T, f_{h2}^*]^T$. Finally, the entire system can be viewed as a cascade of two subsystem systems as in (22), which is ISS by utilizing Lemma 2, and this completes the proof. □

Remark 1: From (18), the coefficient of $\phi_i^2(\tilde{x})$ should be positive in order to have a positive definite V_2. By assuming that K_{D2} and B_{h2} are both diagonal, a lower-bound for the minimum eigenvalue of $K_{D2} + B_{h2}$ ensures the positive definiteness of V_2. On the other hand, from (20) and (21), the parameter β_2 should be positive to conclude the negative definiteness of the derivative of V_2. Hence, another constraint on the minimum eigenvalue of $K_{D2} + B_{h2}$ is imposed to guarantee that the derivative of V_2 is negative definite. By combining these two constraints, the following condition should be satisfied to ensure the stability of the entire system

$$\lambda_{\min}(K_{D2} + B_{h2}) \geq \max\left(\frac{8}{7}\rho, \frac{2\gamma\lambda_{\max}\left(M_{x2}(q_2)\right)}{c}\right) \quad (23)$$

The interpretation of the condition (23) is that, a minimum amount of damping should be displayed by the controller and the operator #2. An important note is that, the required minimum damping is not strict as it depends on the value γ. This condition is simply satisfied for any positive $\lambda_{\min}(K_{D2}+B_{h2})$ by selecting sufficiently small value for the scalar γ. The necessary computations are illustrated in the simulation section.

VI. Simulation and Experimental Results

In this study, both simulation and experimental results are presented to demonstrate the effectiveness of the proposed control scheme. The aim of simulation studies is to investigate the stability and performance of the proposed control approach against a benchmark control architecture proposed in [11]. In order to have a fair comparison between the two controllers, each should be subjected to the same exogenous force inputs, which can only be accomplished in simulations, and not experiments. In both the simulation and experimental studies, two identical Geomagic Touch™ (formerly known as Sensable Phantom Omni) three degree-of-freedom haptic devices are considered as the haptic consoles. The Geomagic Touch has three actuated revolute joints that apply force feedback to the user's hand. This haptic device is widely used in the investigations related to the haptics and telerobotics applications [22]. The haptic device dynamics is presented in [23].

An important consideration for both the simulations and experiments is the environment dynamic model. Owing to its simple structure, the linear Kelvin-Voigt (KV) model is a common environment dynamic model for robotic applications. Nevertheless, the KV model is not physically consistent with the dynamic behaviour of soft tissues. As an example, in the rebound phase before the contact breaks, the KV model predicts an unrealistic sticky force, pulling the robot back in [24]. The nonlinear Hunt–Crossley (HC) contact model introduced in [25], is an alternative approach for representing the dynamic behavior of soft tissue environments displaying limited deformation at the point of contact. HC models have increasingly been used in telerobotic and haptic control systems such as in [24], [26]. According to the HC model, the contact force of the environment is expressed as follows:

$$f_e(t) = \begin{cases} K_e x^n(t) + B_e \dot{x}(t) x^n(t) & x \geq 0 \\ 0 & x < 0 \end{cases}$$

where K_e and B_e are the coefficient of elastic and viscous forces, respectively. The parameter n depends on the physical properties of the environment and is normally between 1 and 2.

A. Simulation Results

In this section, the benchmark controller [11], that involves measured force feedback, is considered for the comparative study. The benchmark proposes a trilateral six channel architecture and the three sides of the system are the haptic console #1, the haptic console #2, and the environment. In the proposed architecture, the desired position and the reflected force of each side is a linear combination of the position and the force of the other two sides. The authority of each user over the task is determined by the dominance factor which is a value between zero and one. A unity dominance factor corresponds to the full authority of the trainer, whereas the dominance factor with the value of zero corresponds to the full authority of the trainee. Note that, our proposed approach is developed for the most primary level of training in which the trainee does not have sufficient experience to perform the operation. Therefore, the dominance factor for the benchmark is set to one in order to have a fair comparison. The response of the haptic system is studied and compared for the above benchmark and the proposed controller based on S-shaped function.

In the simulations, the physical parameters of the operators and the environment are taken from [11] and [24], respectively. The dynamic parameters for the operators' hands are set to $M_{hi} = m_{hi}I$, $B_{hi} = b_{hi}I$, and $K_{hi} = k_{hi}I$ where $m_{hi} = 9\,g$, $b_{hi} = 2N.s/m$, and $k_{hi} = 200N/m$. The parameters for the environment HC model are set to $K_e = 10$, $B_e = 2$, and $n = 1.2$.

As for the controller gains, K_{P1} as explained in Section III should be a positive definite matrix to satisfy the positive definiteness of the Lyapunov function (12). However, this gain is selected small, i.e. $K_{P1} = k_{P1}I$ where $k_{P1} = 1N/m$, to limit the centering force applied to the trainer's hand. On the other hand, the gain K_{P2} directly affects the corrective force applied to the trainee's hand. Therefore, this gain should be chosen sufficiently large to guarantee satisfactory position tracking. Besides, the value of K_{P2} should be considerably larger than the stiffness of the operator's hand denoted by K_{h2} to dominate it. In this investigation, a suitable choice which is considerably larger than K_{h2} is selected as $K_{P2} = k_{P2}I$

This article has been accepted for publication in a future issue of this journal, but has not been fully edited. Content may change prior to final publication. Citation information: DOI 10.1109/TMECH.2019.2917448, IEEE/ASME Transactions on Mechatronics

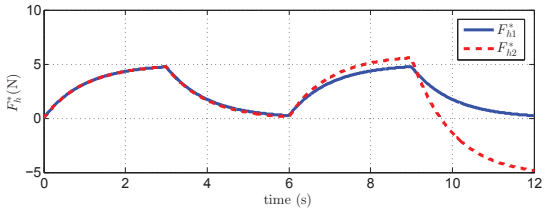

Fig. 3: Exogenous forces applied by operators.

where $k_{P2} = 1250N/m$. Furthermore, K_{D1} and K_{D2} are selected equal to have a similar damping on the haptic consoles. K_{D2} should be selected such that the condition (23) is satisfied. As already explained, the right-hand-side of the inequality (23) depends on the parameter γ, and any positive value can be chosen for this parameter. Therefore, this condition can be satisfied for any positive $\lambda_{\min}(K_{D2} + B_{h2})$ by selecting sufficiently small value for the scalar γ. To mathematically confirm this issue, it is presumed that $\gamma = 0.1$ and the parameter ρ should be obtained such that $\Xi \leq \rho \dot{x}_2$ where Ξ is defined in (19). This can be achieved using the MATLAB constrained optimization routine[1]. The following bounds are considered for the revolute joints in the optimization procedure: $-\frac{\pi}{4} \leq q_{21} \leq \frac{\pi}{4}$, $0 \leq q_{22} \leq \frac{5\pi}{12}$, $0 \leq q_{23} \leq \frac{5\pi}{12}$ where q_{2j} denotes the the jth joint angle of the haptic console #2 for $j = 1, 2, 3$. Note that, the workspace defined by the above bounds is significantly larger than the workspace required in our investigation. The above-mentioned bounds lead to the stability condition $\lambda_{\min}(K_{D2} + B_{h2}) \geq 0.33$. In this study, the derivative gains are set to $K_{D1} = K_{D2} = I$ which satisfies the stability condition (23).

Finally, the parameters of the S-shaped function are set to $\theta_{dz} = 0.5mm$, $\theta_{st} = 2mm$, and $\phi_{dz} = 0.001mm$. Note that the parameters of the controller and the S-shaped function are selected such that the saturation force for the haptic console does not exceed 75% of the output force of the device at the nominal position, which amounts to $2.5N$.

The simulations are obtained using the ode15s solver in Matlab simulink by setting the minimum and maximum sampling times as $0.1ms$ and $4ms$, respectively. For the simulations, a one dimensional path following task in the z direction is considered. The exogenous forces applied by the trainer and the trainee in the z direction are depicted in Fig. 3 with solid (blue) and dashed (red) line, respectively. The trainer's exogenous force is generated by a square wave with the amplitude $5N$, period $6s$, and duty cycle 50% passed through the low-pass filter $1/(s+1)$. The trainee's exogenous force is obtained by perturbing the trainer's exogenous force by 5%, 30%, and 300%, in $t = 3s$, $t = 6s$, and $t = 9s$, respectively.

Fig. 4 shows the simulation results in z direction. The solid (blue) line shows the trainer response, whereas the dashed (red) line represent the trainee's response. The position and force of the benchmark controller [11] are depicted in Fig. 4a, and Fig. 4b with the zoomed plot in Fig. 4c for better comparison. Likewise, the position and the force of the proposed approach are depicted in Fig. 4d and Fig. 4e and the zoomed plot in Fig. 4f.

First, the proposed approach is compared with the benchmark of [11] from the trainer's point of view. Noticeably, a centering force is applied to the trainer haptic console in the proposed approach to ensure ISS stability of the system, while such centering force is not necessary in the approach of [11]. The effect of centering force should be studied by comparing the position of the haptic console #1 as shown in Fig. 4a and Fig. 4d. Owing to the same exogenous forces applied for the implementation of both control architectures, any remarkable affect of the centering force leads to significant difference between the trainer's position in the two methodologies. Nevertheless, as depicted by Fig. 4a and Fig. 4d the trainer's position in the proposed method is not substantially different with the one resulted from the benchmark of [11]. As a result, the centering force does not considerably disturb the trainer's motion. This, as mentioned earlier, is due to the fact that small K_{P1} is needed to guarantee ISS stability which results in negligible centering force.

Next, the effect of the corrective force on the trainee's hands is investigated. From $t = 0s$ to $t = 3s$ the trainee's exogenous forces are exactly the same as that of the trainer's. Hence, the motion of the two haptic consoles are expected to be equal in both cases. This fact is evident in Fig. 4a and Fig. 4d. On the other hand, from $t = 3s$ to $t = 6s$ the trainee's exogenous force is slightly different with the trainer's exogenous force but the position error between the trainer and the trainee does not exceed the safe threshold. This means that the trainee's movements are still in the trusting mode and no compensation force is required in the proposed approach. Note that, in this period, the compensation force is applied to the trainee's hand in the approach of [11], whereas it is not applied in the proposed structure. Nevertheless, the motion of the two haptic consoles are approximately equal in both cases. The key point of the proposed algorithm in the trusting mode is that it allows the trainee to move freely in a safe region without any considerable interference from the trainer. This issue is compliant with the exerted forces depicted in the zoomed figure Fig. 4f. It is apparent that the forces exerted to the surgeons from $t = 3s$ to $t = 6s$ match each other in the proposed structure, whereas these forces are different in the approach of [11].

On the other hand, from $t = 6s$ to $t = 9s$ the exogenous force applied by the trainee and the trainer differ significantly such that the system does not remain in the trusting mode anymore. As a result, the trainee needs guidance from the trainer in the SC case. In this period, the two control structures provide approximately similar behaviors. Furthermore, from $t = 9s$ to $t = 12s$ the difference between the exogenous force applied by the two operators is significantly large, leading to the saturation of the control signal. From Fig. 4e, the control signal of haptic console #2 in the proposed approach after $t \approx 10$ is saturated to avoid damage to the actuators. On the other hand, as Fig. 4b shows, the results of the approach of [11] at this period exceeds the maximum applied force of the considered haptic device.

It is also beneficial to investigate the effect of the parameters

[1]MATLAB function `fmincon` is used in here.

This article has been accepted for publication in a future issue of this journal, but has not been fully edited. Content may change prior to final publication. Citation information: DOI 10.1109/TMECH.2019.2917448, IEEE/ASME Transactions on Mechatronics

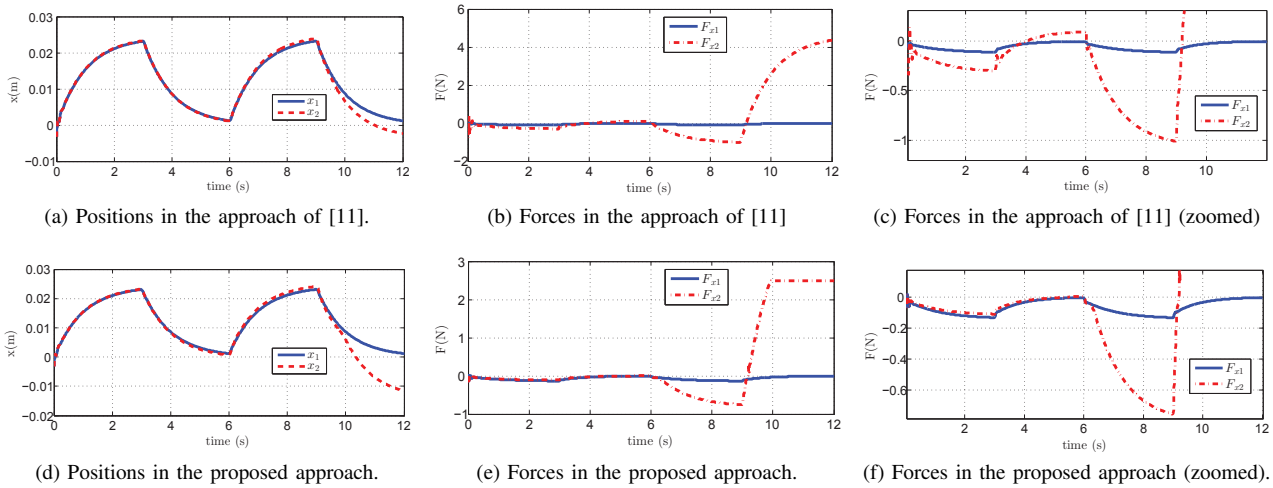

(a) Positions in the approach of [11]. (b) Forces in the approach of [11] (c) Forces in the approach of [11] (zoomed)

(d) Positions in the proposed approach. (e) Forces in the proposed approach. (f) Forces in the proposed approach (zoomed).

Fig. 4: Simulation results in z direction.

θ_{dz}, and ϕ_{dz} on the behavior of the system. For this purpose, the output of s-shaped function is obtained by running the described simulation with various selections of θ_{dz} and ϕ_{dz} while fixing the other parameters. The results are shown in Fig. 5. The solid (blue) line depicts the original case in which $\theta_{dz} = 0.0005$ and $\phi_{dz} = 10^{-6}$. On the other hand, the dashed (red) line shows the output of s-shaped function by setting a smaller value for θ_{dz}; i.e., $\theta_{dz} = 0.0001$. It is expected that a smaller value of θ_{dz} leads to a more limited dead zone. This issue is evident in Fig. 5 as the output of s-shaped function from $t = 3s$ to $t = 6s$ is almost zero for the case $\theta_{dz} = 0.0005$ but is considerable for the case $\theta_{dz} = 0.0001$. Besides, the output of S-shaped function for the case $\theta_{dz} = 0.001$ which is two times of the original case is depicted by dotted (green) line. Generally, the larger the value of θ_{dz}, the more safe region is given to the trainee. This issue is also evident from the figure as the output of s-shaped function for a period of time after $t = 6s$ is zero for the case $\theta_{dz} = 0.001$ but is nonzero for the case $\theta_{dz} = 0.0005$. Finally, the output of S-shaped function for the case that a larger value is set for ϕ_{dz} with respect to the original case; i.e., $\phi_{dz} = 10^{-4}$ is depicted by dashed-dotted (cyan) line. Comparing the results of original case with the last case from $t = 3s$ to $t = 6s$ shows the importance of choosing an appropriate value for $\phi_{dz} = 10^{-4}$. Notwithstanding the fact that the same values of θ_{dz} for the last case with respect to the original case should lead to the same width of dead zone, the larger value of ϕ_{dz} causes the output to become considerable.

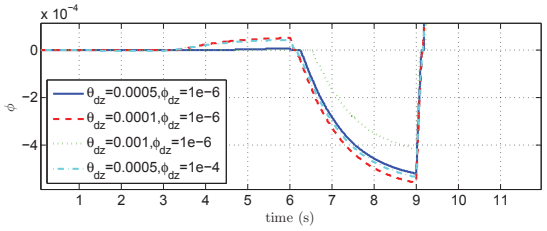

Fig. 5: The effect of changing the parameters of s-shaped function

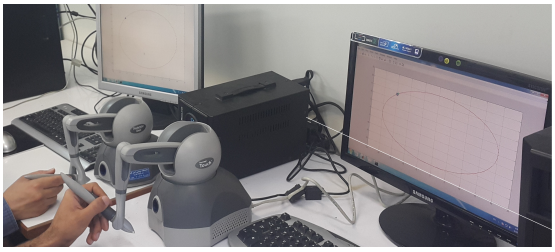

Fig. 6: The experimental setup

B. Experimental Results

The purpose of experiments is to evaluate the response of the proposed methodology in a real haptic system and to investigate the effect of design parameters on the system response. This is mainly investigated through a 2D circular path following task in which the trainer observes her/his own hand position with respect to the circular path in the xy plane on a display, and the trainee observes both her/his own hand position and the trainer's hand position.

Fig. 6 shows the experimental setup utilized to evaluate the proposed control architecture. The system consists of two 3-DOF Geomagic Touch™ devices as the haptic consoles. Data between the haptic consoles is exchanged through a UDP-based communication channel. Similar to the simulation scenario, the haptic console #1 is controlled by the trainer, while haptic the console #2 is held by the trainee. As such, the control laws (7) and (8) are implemented on the haptic consoles #1 and #2, respectively, with the controller parameters are set as that of the simulation parameters. The digital control loop runs at 1kHz.

The trainer and trainee positions and forces, as well as the error between the trainee's and trainer's positions in the x and y directions are depicted in Fig. 7. The total experiment time is $150s$,but in order to have more clear plots, Fig. 7

This article has been accepted for publication in a future issue of this journal, but has not been fully edited. Content may change prior to final publication. Citation information: DOI 10.1109/TMECH.2019.2917448, IEEE/ASME Transactions on Mechatronics

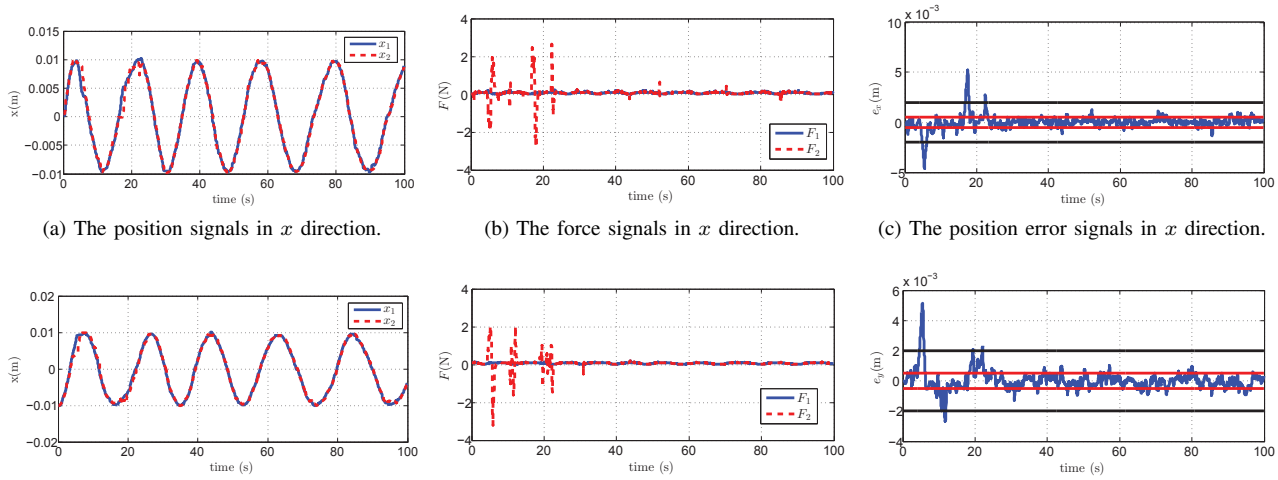

(a) The position signals in x direction. (b) The force signals in x direction. (c) The position error signals in x direction.

(d) The position signals in y direction. (e) The force signals in y direction. (f) The position error signals in y direction.

Fig. 7: Experimental results.

just shows the results from $t = 0s$ to $t = 100s$. In addition, the total 2D motion trajectories of the haptic consoles from $t = 0s$ to $t = 150s$ are shown in Fig. 8. The solid (blue) lines represent the signals related to the trainer, whereas the dashed (red) lines represent the signals corresponding to the trainee. The red lines and the black lines show the bounds of the trusting mode and guidance mode, respectively. As evident from the results, the position of the trainee mostly matches the position of the trainer. In fact, guidance from the haptic system is implemented to steer the trainee to the correct motion. However, at certain times the trainee is requested to cross the safe region for the purpose of investigating the stability of the overall system in the large error mode.

The forces exerted to the operators' hands match well in the trusting mode. This means that the environmental forces are the dominant forces exerted on the hands of the trainer as long as the position error between the trainee and the trainer does not exceed the safe threshold. In the event that the motion error exceeds the safe threshold, the guidance force from the haptic system is applied to the trainee's hand to adjust the trainee's motion.

As it can be seen from the results of x direction in Fig. 7, the corrective force applied to the trainee's hand is notable during the time period $t = 0s$ to $t \approx 25s$. On the other hand, from $t \approx 25s$ to $t = 100s$, the corrective force is only applied at the three instances $t \approx 55s$, $t \approx 67s$, and $t \approx 85s$ for a short period of time and with a small magnitude. Furthermore, from $t = 100s$ to $t = 150s$ the forces reflected to the hands of the trainee and the trainer are approximately similar meaning that the trainee's movements are trusted and little guidance force is necessary. The position error signal in Fig. 7-c clearly shows that at some specific times the position error exceeds the bounds of guidance mode (black lines) and the system goes to large error mode. This situation happens at three periods of time each one last for a few seconds at $t \approx 5s$, $t \approx 15s$, and $t \approx 25s$. As clear from the results, the stability of the system in the large error mode is preserved.

The results of y direction depicted in Fig. 7a may also be similarly interpreted. Clearly, at the beginning of the experiment from $t = 0s$ to $t \approx 25s$ the corrective force is continuously applied to the haptic console #2 to guide the trainee to the right path. Afterwards, from $t = 25s$ to the end of experiment the forces exerted to the haptic console #1 and the haptic console #2 match each other. This implies that little guidance force is needed for the trainee's hands and the trainee's commands are reliable. The position error signal depicts that at some specific periods of time at $t \approx 5s$, $t \approx 10s$, and $t \approx 20s$ the system goes to large error mode. Obviously, the stability of the system in the large error mode is also preserved in the y direction.

The environment is presumed to be soft tissue; therefore, the environment contact force is small. On the other hand, the corrective force should be sufficiently large to dominate the trainee's hand forces. This corrective (coordinating) force depends on the gap between the trainer's and the trainee's hand positions. As the gap grows so does the size of the force. In some parts of the experiment the trainee is asked to deliberately perform wrong movements to generate large position errors. In those parts of the experiment a large force is exerted to the trainee's hand as a guidance force to correct trainee's movements. This issue is also illustrated in the experimental section of the revised manuscript. The time scale in the experimental results has been adjusted.

Furthermore, it can be seen in Fig. 7b and Fig. 7e that the corrective forces are much higher than the environment interaction forces. This is due to the fact the environment models a soft tissue; as such, the environment contact forces are small. On the other hand, the corrective force which depends on the gap between the trainee's and trainer's positions should be sufficiently large to dominate the trainee's hand forces and correct trainee's movements.

The 2D motion trajectories of the haptic consoles depicted in Fig. 8 clearly reveal that the error in trainee's motion is fairly large at the beginning of the training while it is reduced over the time and becomes negligible at the end of experiment.

Next, some experimental results are depicted to show the

This article has been accepted for publication in a future issue of this journal, but has not been fully edited. Content may change prior to final publication. Citation information: DOI 10.1109/TMECH.2019.2917448, IEEE/ASME Transactions on Mechatronics

importance of selecting the appropriate values for the control gains. First, the effect of the stiffness gain of the trainer haptic console controller k_{p1} on the system response is investigated. The aim is to find the maximum value of k_{p1} such that the trainer does not feel the centering force. In two separate experiment, the trainer is asked to go along between two specific points four times and then holds the haptic console at ease such that the minimum possible impedance is exerted by the trainer. Therefore, it is possible to see whether the centering force applied by the haptic console is powerful enough to cause any motion on the haptic device. The positions of haptic consoles are shown in Fig. 9a for the two cases in which $k_{p1} = 10$ and $k_{p1} = 20$. The results show that after exerting minimum impedance at about $t = 30s$, the position of haptic console remain fixed if $k_{p1} = 10$, while it suddenly moves due to the effect of centering force in the case that $k_{p1} = 20$. This means that the value $k_{p1} = 20$ is too high and causes the movement of haptic console. Therefore, an appropriate selection of k_{p1} should be in the range $1 < k_{p1} < 10$ such that the centering force does not cause any unfavorable impact to the trainer's haptic console. Besides, the results through qualitative assessment of the centering force by the trainer corroborates the above quantitative measurement.

In another experiment, the effect of the derivative gain k_{d2} on the stability of the system is analyzed. Similar to the previous case, two experiments are performed such that the all parameters are exactly set as that of the main experiment except the gain k_{d2}. In each experiment, both the trainer and the trainee are asked to move the device between two specific points. At some specific times the trainee is also asked to deliberately make wrong motions such that the system goes to the guidance mode. Next, at each of those times, the trainee is asked to grasps the console by exerting little impedance which leads to minimum damping. The position of trainee haptic console for the case $k_{d1} = k_{d2} = 0.1$ is shown in Fig 9b by dashed-dotted (red) line. In this experiment the trainee deliberately performs wrong movements on about $t = 7s$, $t = 13s$, and $t = 18s$ and then applies minimum force at each of those points. However, no unstable behavior is watched in this experiment by the haptic console. In the event that $k_{d1} = k_{d2} = 0.05$, the results are shown in Fig. 9b by dashed (green) line. In this experiment the trainee moves correctly from $t = 0$ to $t = 7$ but at about $t = 7$ deliberately performs wrong motion and then grasps the haptic device at ease. At that point, a sudden unstable behavior is shown by the trainee haptic console and then the experiment is stopped to avoid damage to the haptic devices. This experiment shows that, as predicted by the stability condition, when the damping values reduce the system tends to show unstable behavior.

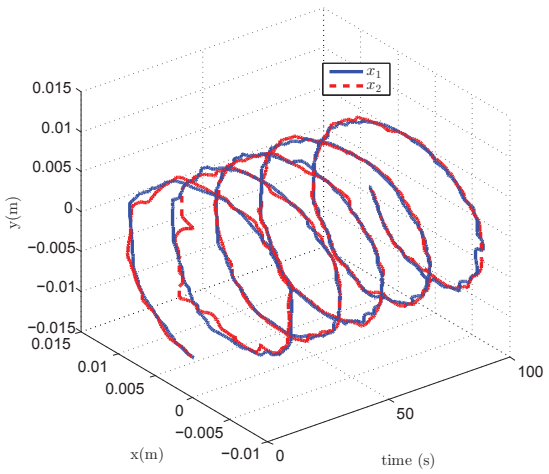

Fig. 8: The 2D motion trajectories of the haptic consoles

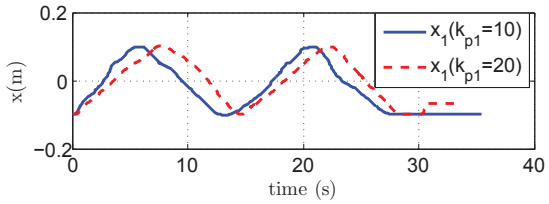

(a) The effect of k_{p1}.

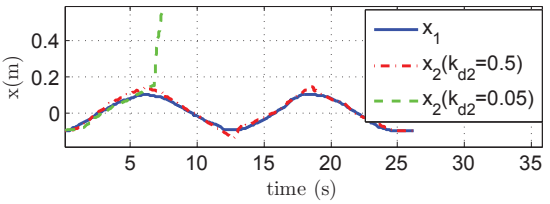

(b) The effect of k_{d2}.

Fig. 9: Effect of changing the control gains on the response

VII. Conclusion and Future Work

In this article, a multilateral control architecture based on a novel S-shaped function is presented for a surgery training haptic system. The corrective force is generated according to the magnitude of motion error of the trainee by utilizing the S-shaped function. In addition, the stability of the closed-loop system is analyzed using the inner product approach and ISS stability theory. Through simulation and experimental results, it is demonstrated that the proposed framework is effective in correcting the trainee's movements.

Future work includes studying the role of shaping function on the stability and kinesthetic performance of the closed-loop system and conducting user studies to poll the opinion of the clinical students and experts and to assess the task performance for specific surgical tasks. Furthermore the effect of delays for tele-haptic training will be analyzed and the time-domain passivity approach (TDPA) for multi-lateral control systems will be considered for guaranteed coupled stability [15].

References

[1] M. D. Kim, K.-H. Lee, S.-M. Lee, J. C. Koo, and S.-H. Ji, "Design and development of a mobile robotic ct system for intraoperative use," *IEEE/ASME Trans. Mechatronics*, 2019.

[2] W. Hong, L. Xie, J. Liu, Y. Sun, K. Li, and H. Wang, "Development of a novel continuum robotic system for maxillary sinus surgery," *IEEE/ASME Trans. Mechatronics*, vol. 23, no. 3, pp. 1226–1237, 2018.

[3] [Online]. Available: http://www.davincisurgery.com/da-vinci-surgery/

[4] T. Endo, A. Kusakabe, Y. Kazama, and H. Kawasaki, "Haptic interface for displaying softness at multiple fingers: Combining a side-faced-type multifingered haptic interface robot and improved softness-display devices," *IEEE/ASME Trans. Mechatronics*, vol. 21, no. 5, pp. 2343–2351, 2016.

[5] C. Basdogan, S. De, J. Kim, M. Muniyandi, H. Kim, and M. A. Srinivasan, "Haptics in minimally invasive surgical simulation and training," *IEEE Comput. Graphics Appl.*, vol. 24, no. 2, pp. 56–64, 2004.

[6] D. Wang, Y. Shi, S. Liu, Y. Zhang, and J. Xiao, "Haptic simulation of organ deformation and hybrid contacts in dental operations," *IEEE Trans. Haptics*, vol. 7, no. 1, pp. 48–60, 2014.

[7] A. M. Tahmasebi, K. Hashtrudi-Zaad, D. Thompson, and P. Abolmaesumi, "A framework for the design of a novel haptic-based medical training simulator," *IEEE Trans. Inf. Technol. Biomed.*, vol. 12, no. 5, pp. 658–666, 2008.

[8] S. Moghimi, S. Sirouspour, and P. Malysz, "Haptic-enabled collaborative training with generalized force and position mappings," in *Symp. Haptic Interfaces Virtual Environ. Teleoperator Syst.*, 2008, pp. 287–294.

[9] K. Razi and K. Hashtrudi-Zaad, "Analysis of coupled stability in multilateral dual-user teleoperation systems," *IEEE Trans. Rob.*, vol. 30, no. 3, pp. 631–641, 2014.

[10] S. S. Nudehi, R. Mukherjee, and M. Ghodoussi, "A shared-control approach to haptic interface design for minimally invasive telesurgical training," *IEEE Trans. Control Syst. Technol.*, vol. 13, no. 4, pp. 588–592, 2005.

[11] B. Khademian and K. Hashtrudi-Zaad, "Dual-user teleoperation systems: New multilateral shared control architecture and kinesthetic performance measures," *IEEE/ASME Trans. Mechatronics*, vol. 17, no. 5, pp. 895–906, 2012.

[12] M. Shahbazi, S. Atashzar, H. Talebi, and R. Patel, "Novel cooperative teleoperation framework: Multi-master single-slave system," *IEEE/ASME Trans. Mechatronics*, vol. 20, no. 4, pp. 1668–1679, Aug 2015.

[13] M. Shahbazi, S. F. Atashzar, H. A. Talebi, and R. V. Patel, "An expertise-oriented training framework for robotics-assisted surgery," in *Proc. IEEE Int. Conf. Rob. Autom.*, 2014, pp. 5902–5907.

[14] M. Panzirsch, J. Artigas, A. Tobergte, P. Kotyczka, C. Preusche, A. Albu-Schaeffer, and G. Hirzinger, "A peer-to-peer trilateral passivity control for delayed collaborative teleoperation," in *International Conference on Human Haptic Sensing and Touch Enabled Computer Applications*. Springer, 2012, pp. 395–406.

[15] H. Van Quang and J.-H. Ryu, "Stable multilateral teleoperation with time domain passivity approach," in *Intelligent Robots and Systems (IROS), 2013 IEEE/RSJ International Conference on*, 2013, pp. 5890–5895.

[16] C. C. de Wit, B. Siciliano, and G. Bastin, *Theory of robot control*. Springer Science & Business Media, 2012.

[17] M. Vukobratovic, D. Surdilovic, Y. Ekalo, and D. Katic, *Dynamics and robust control of robot-environment interaction*. World Scientific, 2009.

[18] M. Shahbazi, S. F. Atashzar, M. Tavakoli, and R. V. Patel, "Position-force domain passivity of the human arm in telerobotic systems," *IEEE/ASME Trans. Mechatronics*, 2018.

[19] S. Arimoto, *Control Theory of Nonlinear Mechanical Systems*. Oxford University Press, Inc., 1996.

[20] H. J. Marquez, *Nonlinear control systems: analysis and design*. John Wiley & Sons, Inc., 2003.

[21] H. L. Royden and P. Fitzpatrick, *Real Analysis. 4th*. Boston, MA: Prentice Hall, 2010.

[22] H. Culbertson and K. J. Kuchenbecker, "Ungrounded haptic augmented reality system for displaying roughness and friction," *IEEE/ASME Trans. Mechatronics*, vol. 22, no. 4, pp. 1839–1849, 2017.

[23] E. Naerum, J. Cornella, and O. J. Elle, "Contact force estimation for backdrivable robotic manipulators with coupled friction," in *Proc. IEEE/RSJ Int. Conf. Intell. Robots Syst.*, 2008, pp. 3021–3027.

[24] A. Haddadi and K. Hashtrudi-Zaad, "Online contact impedance identification for robotic systems," in *Proc. IEEE/RSJ Int. Conf. Intell. Robots Syst.*, 2008, pp. 974–980.

[25] K. Hunt and F. Crossley, "Coefficient of restitution interpreted as damping in vibroimpact," *ASME J. Appl. Mech.*, vol. 42, 1975.

[26] A. Achhammer, C. Weber, A. Peer, and M. Buss, "Improvement of model-mediated teleoperation using a new hybrid environment estimation technique," in *Proc. IEEE Int. Conf. Rob. Autom.*, 2010, pp. 5358–5363.

Mohammad Motaharifar received the B.Sc. degree in electrical engineering from the Iran University of Science and Technology, Tehran, Iran, in 2009, and the M.Sc. degree in electrical engineering from the Amirkabir University of Technology, Tehran, in 2011. He was a Research Assistant at Real time Systems Laboratory, Electrical Engineering Department, Amirkabir University of Technology from 2011 to 2014. He is currently working toward the Ph.D. degree from the K. N. Toosi University of Technology, Tehran. He was a visiting research assistant at the Department of Electrical and Computer Engineering, Queens University, Kingston, ON, Canada from September to December 2018. His research interests include medical robotics, nonlinear control, and robust control.

Hamid D. Taghirad (SM12) received the B.Sc. degree in mechanical engineering from Sharif University of Technology, Tehran, Iran, in 1989 and the M.Sc. degree in mechanical engineering and the Ph.D. degree in electrical engineering from McGill University, Montreal, QC, Canada, in 1993 and 1997, respectively. He is currently a Professor and the Vice Chancellor for Global Strategies and International Affairs and the Director of the Advanced Robotics and Automated System, K.N. Toosi University of Technology, Tehran. His publications include five books and more than 190 papers in international journals and conference proceedings. His research interests include robust and nonlinear control applied to robotic systems. Dr. Taghirad is the Chairman of the IEEE control system chapter in the Iran section, a member of the board of the Industrial Control Center of Excellence, K. N. Toosi University of Technology. He is the Editor-in-Chief of Mechatronics Magazine and a member of the editorial board of International Journal of Robotics: Theory and Application and International Journal of Advanced Robotic Systems. His research interest includes robust and nonlinear control applied to robotic systems.

Keyvan Hashtrudi-Zaad (SM08) received the Ph.D. degree in electrical and computer engineering from the University of British Columbia, Vancouver, BC, Canada, in 2000. He then held a consulting position with Motion Metrics International Corporation, Vancouver, where he worked on the development of a dynamic payload monitoring system for heavy duty hydraulic machines. In 2001, he joined the Department of Electrical and Computer Engineering, Queens University, Kingston, ON, Canada, where he is currently a Professor and the Co-director of BioRobotics Research Laboratory. His research interests include telerobotics, haptics, Tele-rehabilitation, autonomous driving, and control systems. Dr. Hashtrudi-Zaad served as an Associate Editor of the IEEE TRANSACTIONS ON HAPTICS and on the organization committees of a number of IEEE-sponsored conferences.

Seyed Farzad Mohammadi received the fellowship degree in anterior segment of the eye from Tehran University of Medical Sciences, Tehran, Iran, in 2007. He is currently an Associate Professor of Ophthalmology at Translational Ophthalmology Research Center, Farabi Eye Hospital, Tehran University of Medical Sciences, Tehran, Iran. Dr. Mohammadi is Board-certified in Ophthalmology and Fellow of International Council of Ophthalmology. In recent years, he has been focused on visual optics, refractive surgery, academic ophthalmology and leadership, ophthalmic nursing and qualitative research, and vision-related quality of life.

Figure Captions:

Fig. 1: The haptic system for surgery training.
Fig. 2: The S-shaped function, $\phi(\theta)$.
Fig. 3: Exogenous forces applied by operators.
Fig. 4: Simulation results in z direction.
Fig. 5: The effect of changing the parameters of s-shaped function
Fig. 6: The experimental setup.
Fig. 7: Experimental results
Fig. 8: The 2D motion trajectories of the haptic consoles
Fig. 9: Effect of changing the control gains on the response